Anti-Tumorigenic Properties of Omega-3 Endocannabinoid Epoxides

Journal:	*Journal of Medicinal Chemistry*
Manuscript ID	jm-2018-002437.R4
Manuscript Type:	Article
Date Submitted by the Author:	23-May-2018
Complete List of Authors:	Roy, Jahnabi; University of Illinois, Urbana- Champaign, Chemistry Watson, Josephine; University of Illinois Urbana Champaign, Comparative Biosciences Hong, Insup; University of Illinois Urbana Champaign, Comparative Biosciences Fan, Timothy; University of Illinois at Urbana-Champaign, Department of Veterinary Clinical Medicine Das, Aditi; University of Illinois Urbana Champaign, Comparative Biosciences

Anti-Tumorigenic Properties of Omega-3 Endocannabinoid Epoxides

Jahnabi Roy[a], Josephine Watson[b], Insup Hong[†], Timothy M. Fan[‡] and Aditi Das[†,b,c]*

[†]Department of Comparative Biosciences, [‡]Department of Veterinary Clinical Medicine [a] Department of Chemistry, [b] Department of Biochemistry; [c] Beckman Institute for Advanced Science, Division of Nutritional Sciences, Neuroscience Program and Department of Bioengineering, University of Illinois Urbana–Champaign, Urbana IL 61802, USA

Correspondence to: Aditi Das, aditidas@illinois.edu

KEYWORDS

Osteosarcoma, Omega-3 fatty acids, endocannabinoids, cannabinoid receptor

ABSTRACT

Accumulating studies have linked inflammation to tumor progression. Dietary omega-3 fatty acids including docosahexaenoic acid (DHA) have been shown to suppress tumor growth through their conversion to epoxide metabolites. Alternatively, DHA is converted enzymatically into docosahexaenoylethanolamide (DHEA), an endocannabinoid with anti-proliferative activity. Recently, we reported a novel class of anti-inflammatory DHEA-epoxides (EDP-EAs) that contain both ethanolamide and epoxide moieties. Herein we evaluate the anti-tumorigenic properties of EDP-EAs in an osteosarcoma model. First, we show ~80% increase in EDP-EAs in metastatic lungs versus normal mouse lungs. We found significant differences in the apoptotic and anti-migratory potency of the different EDP-EA regioisomers, which are partly mediated

through cannabinoid receptor 1 (CB1). Furthermore, we synthesized derivatives of the most pro-apoptotic regioisomer. These derivatives had reduced hydrolytic susceptibility to fatty acid-amide hydrolase and increased CB1 binding. Collectively, we report a novel class of EDP-EAs that exhibit anti-angiogenic, anti-tumorigenic and anti-migratory properties in osteosarcoma.

INTRODUCTION

Recent studies in cancer have focused on understanding the role of inflammation in tumor initiation and malignant progression. It has been shown previously that inflammatory conditions can promote oncogenic transformation. In addition, the carcinogenic milieu can also generate an inflammatory microenvironment, which favors tumor progression. [1-3] Dietary omega-3 fatty acids such as eicosapentaenoic acid (EPA) and docosahexaenoic acid (DHA) have been shown to suppress tumor growth and progression through their conversion to anti-inflammatory, pro-resolving and anti-tumorigenic lipids. [4 5 6 7] As inflammation can promote tumor initiation, proliferation, and progression, it is hypothesized that omega-3 fatty acid derived lipid metabolites prevent tumor formation and metastasis in a multifaceted manner. [5] Hence, there is biological and clinical justification to discover if potential omega-3 fatty acid derived lipid metabolites possess anti-tumorigenic and anti-inflammatory properties.

Cytochrome P450 (CYP) epoxygenases convert omega-3 fatty acids such as EPA and DHA into epoxides that exhibit anti-cancer properties. Specifically, the EPA-epoxides are anti-proliferative.[8] In addition, the terminal epoxide of EPA, 17,18-epoxyeicosatetraenoic acid (17,18-EEQ), decreased endothelial cell proliferation, interrupted the cell cycle in S-phase and down-regulated the cyclin D1/cyclin-dependent kinase (CDK)-4 complex. The corresponding DHA epoxide, epoxydocosapentaenoic (EDP) inhibits metastasis and tumor growth.[9]

Furthermore, the action of the DHA and EPA epoxides are attenuated in the absence of a soluble epoxide hydrolase (sEH) inhibitor, indicating that the functional epoxide moiety is key for their anti-tumorigenic properties.

Omega-3 fatty acids such as DHA and EPA are also converted enzymatically into docosahexaenoyl ethanolamide (DHEA) and eicosapentaenoyl ethanolamide (EPEA) through the N-acyl ethanolamine synthesis pathway similar to the conversion of arachidonic acid to arachidonoyl ethanolamide (AEA, anandamide). [10, 11] These ethanolamide derivatives are collectively termed as endocannabinoids (eCBs) as they elicit similar physiological effects as cannabinoids found in cannabis. The endocannabinoid system consists of the biosynthetic and degradative enzymes, including diacylglycerol lipase and fatty acid amide hydrolase, [12] the eCBs, anandamide and 2-arachidonylglycerol, and the cannabinoids receptors 1 and 2 (CB1 & CB2). [13, 14] While, CB1 is predominantly found in the central nervous system (CNS), CB2 is found in immune cells. [15] These receptors interact with various eCBs to exert their physiological activities. [16] Interestingly, these receptors interact with the active components of cannabis, and are responsible for cannabis' psychoactive and anti-inflammatory properties. Phytocannabinoids, Δ-9-THC and cannabidiol (CBD), are two specific components of cannabis that have been shown to induce apoptosis in hepatocellular carcinoma, breast cancer and colon cancer.[17] As a whole, the phytocannabinoids and eCBs have been shown to play a powerful role in cancer cell proliferation, apoptosis, inflammation and immunomodulation.[18, 19]

The most studied eCBs in the human body are AEA and 2-arachidonylglycerol (2-AG) that are derived from the omega-6 fatty acid arachidonic acid (AA). Anandamide was shown to be anti-tumorigenic in breast cancer, colorectal cancer as well as osteosarcoma. [20-23] 2-AG has been shown to induce apoptosis in prostate cancer. [24] Omega-3 derived eCBs, DHEA and EPEA have

shown greater anti-proliferative activity than their parent counterparts in prostate cancer cells.[11] Additionally, it was also shown that the activity of eCBs in cancer cells was increased in the presence of a fatty acid amide hydrolase (FAAH) inhibitor, indicating that the ethanolamide endocannabinoids, AEA DHEA and EPEA contributes to the increased pro-apoptotic and anti-proliferative activity. [10, 11]

Recently, we showed that a novel class of eCB epoxides are generated from the cross-talk of the NAPE-PLD pathway and CYP epoxygenase pathways that were found in multiple tissues [25] (Figure 1a). These bi-functional metabolites contain both ethanolamide and epoxide motifs that function through different signaling pathways leading to several overlapping physiological outcomes. Both the eCB and epoxyeicosanoid pathway have been implicated in cancer as described above. [8, 9] Hence, we wanted to evaluate their anti-tumorigenic properties of dual functional eCB epoxides in a cancer model. These lipid metabolites termed as EPEA epoxide (a.k.a. epoxyeicosatetraenoic-ethanolamide (EEQ-EA)) and DHEA epoxide (a.k.a. epoxydocosapentaenoic-ethanolamide (EDP-EA)) are synthesized from EPEA and DHEA by cytochrome P450s and are anti-inflammatory and vasodilatory in nature. More importantly, the DHEA epoxides are widely distributed throughout the body. Additionally, herein we show that there is an ~80% increase in these levels in metastatic lungs (Figure 1b and figure S1) as compared to lungs of normal mice. This indicates that they might play a physiological role in tumorigenesis and cancer metastasis.

Herein, we investigate the anti-tumorigenic activities of the different regioisomers of DHEA epoxides on osteosarcoma cells. Osteosarcoma (OS) is the most common primary bone cancer in humans and presents high rates of invasion and metastasis. The cannabinoid receptor agonist WIN-55212 has been shown to potentiate the anti-tumorigenic properties of drugs like

adriamycin in OS. [26] Additionally, the administration of cannabinoid receptor agonists have shown to reduce bone loss in bone tumor models and cannabinoid receptor mediated nociceptive pain. [27, 28] Taken together, herein we will show that DHEA epoxide regioisomers and their stable derivatives will exhibit anti-tumorigenic activities in osteosarcoma and will potentially reduce bone cancer pain through receptor selective activation.

In order to examine the anti-tumorigenic properties of DHEA epoxides, we will first test the apoptotic potential of the different regioisomers of DHEA epoxides using Annexin V staining assay in three different OS cell lines - metastatic OS cell lines MG63 and 143B and the non-metastatic cell line HOS, and identified the most potent DHEA epoxide regioisomer. We further tested the anti-migratory potential of the DHEA epoxides via a wound healing assay in all three cell lines.[29] Interestingly, we observed significant differences between the different DHEA epoxide regioisomers tested with respect to their pro-apoptotic and anti-migratory properties that were uniform across the different OS cell lines chosen for the studies indicating that the specific isomers of these lipid metabolites triggered common signaling pathways.

Furthermore, we synthesized stable derivatives of the most pro-apoptotic regioisomer of DHEA epoxide (10,11-EDP-EA) to reduce its hydrolytic susceptibility to fatty acid-amide hydrolase (FAAH) and increase binding to cannabinoid receptor 1 (CB1). The the most potent regioisomer and its stable derivatives were further tested towards their anti-tumorigenic, anti-migratory and FAAH hydrolysis.

Collectively, we report a novel class of DHEA-epoxides and their stable derivatives that exhibit anti-inflammatory,[30] anti-angiogenic, anti-tumorigenic and anti-migratory properties and by virtue of their ability to bind cannabinoid receptors might reduce nociceptive bone pain in

osteosarcoma. As osteosarcoma is accompanied by inflammation and pain, these molecules could aid in alleviating both.

RESULTS

DHEA epoxides are endogenously produced in osteosarcoma metastatic lung tissues. We developed a targeted lipidomics method using LC-MS/MS in multiple reaction monitoring (MRM) mode to identify and quantitate DHEA epoxides (EDP-EA) regioisomers (19,20-, 16,17-, 13,14-, 10,11-, and 7,8-). [30] In order to quantify basal levels of endogenous EDP-EA regioisomers in metastatic and non-metastatic lungs, we measured these metabolites in mice with osteosarcoma. Next, we used a metastatic tumor model to show. Specifically, 10^6 K7M2 cells (murine OS cells) were prepared in HBSS and intravenously injected into the tail vein of 6−8 week old female BALB/c mice in a 200 μL volume. Lungs from ten mice, five mice with lungs free of tumor and five with lung metastasized osteosarcoma tumors were isolated and the total endocannabinoids were extracted and quantified by LC-MS/MS as described in materials and methods. As indicated in figure 1b and figure S1, we can observe that both tumor-free lungs in mice where no OS was induced, and lungs with tumors produced eCB epoxides with several fold difference compared to DHEA, the parent molecule. There was ~87% increase in the terminal DHEA epoxide (19,20-EDP-EA), 66% increase in 16,17-EDP-EA, 72% increase 13,14-EDP-EA, 49% increase 10,11-EDP-EA in lungs with metastatic tumor burden, while DHEA was not different in lung tissue with metastatic burden as compared to healthy lungs with no tumors. The high increase of these metabolites in the metastasized lungs warranted further investigation whether they were promoting tumor or they exhibit anti-tumorigenic properties. Previously, we have shown that these metabolites are anti-inflammatory. [30]

In order to investigate the effects of eCB epoxides on osteosarcoma, all five regioisomers were synthesized as described previously. [25] Briefly, mCPBA was used to oxidize DHA, and the epoxide regioisomers were purified using reverse and normal phase HPLC. The individual regioisomers were coupled to ethanolamine and purified by reverse phase chromatography. The compounds were quantified using synthesized standards and used for further studies.

Effect of DHEA epoxides (EDP-EA) regioisomers on cell viability.

To evaluate the effect of EDP-EA isomers on cellular viability of osteosarcoma cells, cell titer blue (CTB) assay was performed on 143B metastatic OS cells at 5 μM concentration. The cell titer blue assay measures cellular viability by measuring the conversion of dye reazurin into fluorescent end product resorufin by living cells. The fluorescence produced is directly proportional to the viable cells. As seen in Figure 1c only 13,14-, 10,11- and 7,8- EDP-EA reduced total cell viability at 12.5 μM concentration and 19,20-EDP-EA and 16,17-EDP-EA were less effective. All regioisomers were tested for their effect on 143B cell's viability by cell titer blue (CTB) assay at various concentrations as seen in figure S2. However, at 25 μM concentration, complete reduction of cell viability was observed for all EDP-EA isomers. Since 7,8-, 10,11- and 13,14- were more effective at reducing cell viability than the other two regioisomers at lower concentrations, their apoptotic and anti-migratory potential was further evaluated. In order to evaluate if the decrease in cell viability of the three different DHEA epoxide regioisomers is due to cell death or check in cell migration, we performed apoptosis and cell migration assay.

Induction of apoptosis in metastatic OS cells by DHEA epoxides (EDP-EA) regioisomers

The apoptotic potential of 7,8-EDP-EA, 10,11- EDP-EA and 13,14-EDP-EA were tested in three different cell lines - HOS, 143B and MG63 cells using the Annexin V/ PI staining assay at 12.5 μM concentration. This concentration was chosen to reflect a point in the CTB assay where cell viability is reduced but not completely diminished. The Annexin V/ PI binding assay measures apoptotic cells by binding labeled annexin V to phosphatidylserine (PS) species. PS is an inner leaflet lipid that flips to the outer leaflet of the plasma membrane in apoptotic cells. The fluorescence by annexin V is proportional to apoptotic cells. PI binds to DNA in necrotic cells. A signal from both annexin V and PI indicate cells in late apoptosis. As seen in Figure 1d, all three regioisomers induced apoptosis in all the cell lines at a concentration of 12.5 μM. Specifically, in 143B cell line (Table ST3), 7,8-EDP-EA induced 8.75 ±0.1% apoptosis (p=0.001). 10,11-EDP-EA induced 17.92 ± 3.3% (p=0.05) apoptosis and 13,14- EDP-EA induced 9.9 ± 1.9% apoptosis (p=0.09). Similar to these results, in MG63 cells (Table ST4), 7,8-EDP-EA induced 16.4 ±1.4% apoptosis (p=0.011). 10,11-EDP-EA induced 26.6 ± 3.5% (p=0.027) apoptosis and 13,14- EDP-EA induced 16.9 ± 2.3% (p=0.04) apoptosis. In HOS cells (Table ST2), the trend followed and 7,8-EDP-EA 17.1± 0.5% apoptosis (p=0.023 as compared to control). 10,11-EDP-EA induced 31.1 ± 2.3% apoptosis (p=0.007) and 13,14- EDP-EA induced 19.6 ± 3.5% apoptosis (p=0.027). In contrast to these results, treatment of all three different cell lines with AA, AEA, DHA and DHEA at 12.5 μM concentration showed no induction of apoptosis as compared to no treatment control (Table ST1).

DHEA epoxides inhibit cell migration of cancer cells determined using wound healing assay

The wound healing assay has been shown to be an effective measure for directional migration of cells *in vivo.* [31] This assay measures the migration of cells across a scratch or wound over time as an indicator of cell migratory potential. A wound healing assay was performed for 7,8-EDP-EA,

10,11- EDP-EA and 13,14-EDP-EA at 5 μM. This concentration was chosen to reflect a concentration where the compounds are not significantly pro-apoptotic and the reduction in wound healing would be due to the compound's anti-migratory properties only. Figure 1e is representative of the effects of 7,8-EDP-EA, 10,11- EDP-EA and 13,14-EDP-EA on the wound closure in 143B cells. Figure 1f represents the ratio of wound remaining in the treatment to the wound remaining in no treatment control at three time points, 0h, 6h and 10h. Therefore a ratio of 1 indicates that same percentage area of wound remains in treatment and control and thus treatment is no different than control. A ratio higher than 1 indicates that the treatment has higher percentage area of wound remaining and thus a compound that restricts migration. As seen from the data in Figure 1f, in HOS cells, all three compounds inhibit cell migration to an extent. For 7,8-EDP-EA (at 6h $p=0.07$ and at 10h $p=0.35$) and 13,14-EDP-EA (at 6h $p=0.5$ and at 10h, $p=0.4$) the difference in wound closure at 10 hours is not significant. For 10,11-EDP-EA, the wound closure at 10 hours is 1.5 times better than in control (at 6h, $p=0.08$ and at 10h, $p=0.17$). In 143B cells, Figure 1f, 7,8-EDP-EA and 13,14-EDP-EA do not inhibit wound healing at 10 hours. However 10,11-EDP-EA inhibits wound closure significantly (at 6h $p=0.21$ and at 10h $p=0.05$). In MG63 cell lines, Figure 1f, all three isomers restrict wound healing and at 10 hours and 10,11-EDP-EA inhibited wound closure with 10,11-EDP-EA being twice as much as the control (at 6h $p=0.38$ and at 10h $p=0.06$). For 13,14-EDP-EA the wound was restricted at 10h but not at 6h (at 6h $p=0.018$ and at 10h $p=0.015$). For 7,8-EDP-EA a similar trend was seen with $p= 0.23$ at 6h and $p=0.23$ at 10h. Thus, while all three isomers in most conditions demonstrate variable capacity to restrict wound healing and thereby show anti-migratory potential, the directional trend effect is greatest in 10,11-EDP-EA.

From our apoptosis and wound healing assays, 10,11-EDP-EA was the most potent regioisomer. This was partly mediated through cannabinoid receptor 1 as the reduction of cell migration by 10,11-EDP-EA in the 143B cell line was completely abolished using CB1 receptor antagonist rimonabant (Supplementary Figure S4). [32]

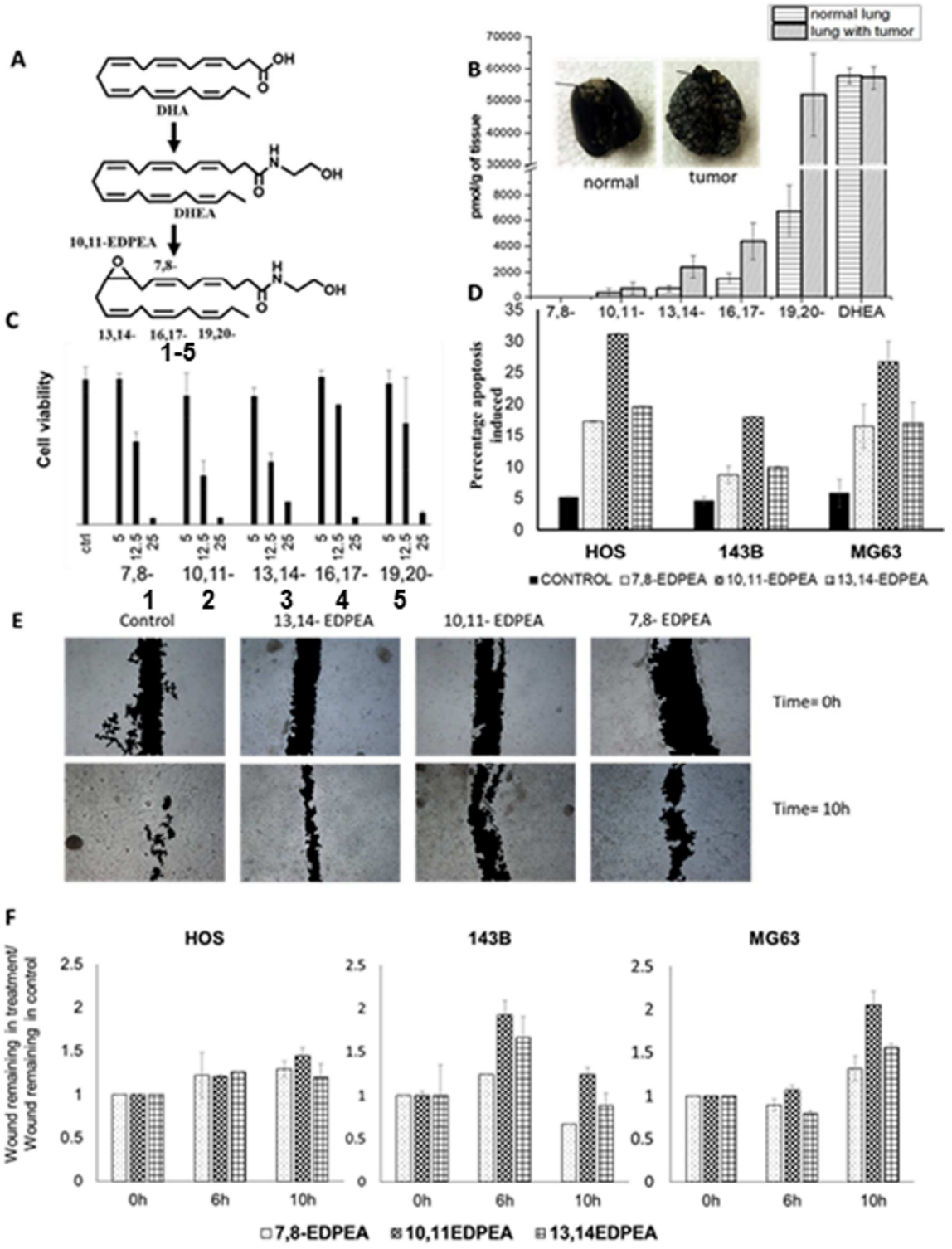

Figure 1: (A) Synthesis of DHEA-epoxide regioisomers- 19,20-(5), 16,17-(4), 13,14-(3), 10,11-(2) and 7,8- EDP-EA (1). **(B)** The levels of endocannabinoid epoxides of DHEA and DHEA

epoxides in normal lungs and lungs of mice with tumor metastasis. Lungs in image were infused with India ink and white lesions represent metastatic tumor burden **(C)** Percentage cell viability as measured by cell titer blue assay by various regioisomers at 5 μM, 12.5 μM and 25 μM. **(D)** Apoptosis induced in HOS, 143B and MG63 cells at 12.5 μM concentration of 13,14-EDP-EA (crisscross), 10,11- EDP-EA (checkered) and 7,8- EDP-EA (dots). **(E)** Wound healing scratch shown at 0h and 10h in 143B cell lines by 13,14-EDP-EA 10,11- EDP-EA and 7,8- EDP-EA at 5 μM concentration. **(F)** Wound healing represented as a ratio of wound remaining in treatment and wound remaining in control over 10 hours in three cell lines (i) HOS, (ii) 143B and (iii) MG63 by 5 μM concentration of 13,14-EDP-EA (crisscross), 10,11- EDP-EA (checkered) and 7,8- EDP-EA (dots).

Synthesis of amide derivatives of 10,11-DHEA epoxide (10,11-EDP-EA)

The eCB epoxides are dual functional molecules. As the amide bond is susceptible to fatty acid amide hydrolase (FAAH), we designed more stable analogs of 10,11-EDP-EA, which shows highest efficacy amongst the various epoxide derivatives of DHA. Derivatives were made at the carboxylate end for different amide modifications, to reduce susceptibility to FAAH as well as better receptor binding to CB1 and CB2, which are the purported receptors for apoptotic activity.

The current literature has mainly focused on anandamide or arachidonylethanolamine (AEA) derivatives, since AEA is the biological ligand of CB1 and CB2 receptors and thus is likely to be the receptor binding to DHEA and its analogs. It has been previously shown that introduction of a methyl group at the 1' position of the amide results in increased metabolic stability of AEA, while affecting the CB1 binding ability [33]. It was shown that the R isomer shows 4-fold higher CB1 binding and the S isomers shows 2-fold lower binding as compared to AEA. Thus the R-1'-methyl isomer was the first modification made to 10,11-EDP as 10,11-EDP-IA (figure 2a). Next,

the cyclopropyl derivative of AEA has been shown to have modest FAAH inhibition with an IC_{50} value of 4.1 ±2.0 μM, with significantly increased CB1 binding [34] thus 10,11-EDP-CA was prepared. Finally, the n-propyl derivative (10,11-EDP-NA) was made to assess the effect of acyl chain length on FAAH hydrolysis. It has also been shown to have better affinity for CB1 as compared to AEA. [35, 36]

The synthesis of these analogs is outlined in the materials and methods section and shown in Figure 2a similar to the synthesis of 10,11-EDP-EA. Briefly, 10,11-EDP was incubated with NHS and EDC in acetonitrile for 20 mins at 37 °C, followed by additional of the corresponding amine and stirring overnight at room temperature. The amines were purified by reverse phase HPLC chromatography and quantified similar to 10,11-EDP-EA.

Susceptibility to FAAH hydrolysis of 10,11-DHEA epoxides and its amide derivatives

Fatty acid amide hydrolase (FAAH) is a ubiquitously expressed protein in various mammals and the sequence of the protein has shown to be highly conserved in humans, [37] mouse [37] and pig [38]. For our studies, we used pig brain membrane preparations to analyze the effect of FAAH on 10,11-EDP-EA as well as the three amino derived modifications. [39] The products of hydrolysis were measured by LC-MS/MS as indicated in materials and methods section. As observed from figure 2b, there was significant reduction of hydrolytic potential in all the three derivatives as compared to 10,11-EDP-EA ($p<0.01$). While the rate of hydrolysis of 10,11-EDP-EA to 10,11-EDP was 30.0 ± 0.3 pmol min^{-1} mg $protein^{-1}$, the rate of hydrolysis for the derivatives - 10,11-EDP-NA, 10,11-EDP-IA and 10,11-EDP-CA was 0.09 ± 0.01 pmol min^{-1} mg $protein^{-1}$ 0.99 ± 0.04 pmol min^{-1} mg $protein^{-1}$and 5.17 ± 0.06 pmol min^{-1} mg $protein^{-1}$ respectively. For 19,20-EDP-EA, the rate is 150 pmol min^{-1} mg $protein^{-1}$. [25] Since the three derivatives show significantly

reduced hydrolytic susceptibility, they could have higher bioavailability and thus their apoptotic and anti-migratory potential was further evaluated.

Apoptosis induced by amino modified derivatives of 10,11 DHEA epoxide (10,11-EDP-EA)

All three amino-modified derivatives of 10,11-EDP were tested for their apoptotic activity by Annexin V/ PI binding assay. All three compounds showed increased apoptotic potential as compared to the no treatment vehicle control (Figure 2c). The cyclopropyl analog had the highest pro-apoptotic potential among the three derivatives. In HOS, MG63 and 143B cells, it increased apoptosis to 27.2 ± 4.1% (p= 0.036 as compared to control), 17.1 ± 4.4% (p= 0.078 as compared to control) and 21.3 ± 1.9% (p=0.01) respectively. The iso-propyl analog was the second most effective in HOS and MG63 cells with apoptotic potentials of 20.2± 1.8% (p= 0.016 as compared to control) and 17.5 ± 2.8% (p= 0.033 as compared to control) respectively. In 143B cells it was only 18.8 ± 0.3% (p=0.0004) for the iso-propyl derivative as compared to 25.7 ± 0.4% (p=0.0002) for the n-propyl derivative. However, the n-propyl derivative was least effective in HOS and MG63 cells with only 17.1 ± 1.4% (p= 0.017 as compared to control) and 15.2 ± 3.3% (p= 0.06 as compared to control) respectively. Overall, all the derivatives showed similar pro-apoptotic potential to the parent compound without discernable differences.

Wound healing assay to determine the potential to inhibit cell migration by amino modified derivatives of 10,11 DHEA epoxide (10,11-EDP-EA)

A wound healing assay was used to analyze the anti-migratory properties of the three derivatives. The data in Figure 2d are represented as a ratio of the percentage area remaining in the wound by compound and the control. As seen in Figure 2d, in all the cell lines, all the 10,11-EDP

derivatives restrict wound healing at 10 hours. Among the derivatives, the 10,11-cyclopropyl derivative shows significantly greater potency at the 6 and 10 hour time points inhibiting migration by 4.5- 6 times more than vehicle control (at 6 hours p= 0.19 for 143B cells, p= 0.57 for HOS cells and at 10 h, p= 0.11 for 143B cells, p= 0.37 for HOS cells). Similarly as seen in figure 2d, in the 143B and HOS cells, restriction in wound healing was 1- 1.9 times by 10,11-EDP-EA (for HOS cells at 6h, p=0.08 and at 10h, p=0.17 and 143B cells at 6h, p=0.21 and at 10h, p=0.05), 1- 1.47 times by n-propyl derivative (for HOS cells at 6h, p=0.39 and at 10h, p=0.44 and 143B cells at 6h, p=0.4 and at 10h, p=0.0002), 1- 3.9 times by isopropyl derivative (for HOS cells at 6h, p=0.58 and at 10h, p=0.99 and 143B cells at 6h, p=0.059 and at 10h, p=0.002). Finally, in the MG63 cell line (figure 2d), the restriction in wound healing was 1-2 times by 10,11-EDP-EA (at 6h p=0.38 and at 10h p=0.06) as compared to the control. The 10,11-EDP-NA (at 6h, p=0.7 and at 10h, p=0.94) and 10,11-EDP-IA (at 6h, p=0.57 and at 10h, p=0.34) were slightly poorer than the control in restricting cell migration. 10,11-EDP-CA (at 6h p= 0.12 and at 10h p=0.09 as compared to vehicle control and p>0.9 as compared to 10,11-EDP-EA) was comparable to 10,11-EDP-EA for the MG63 cell line in restricting cell migration. As observed from the various results, it was concluded that the 10,11-EDP-CA was the most potent in inhibiting wound healing in 143B and HOS cells and comparable to the parent molecule in MG63 cells.

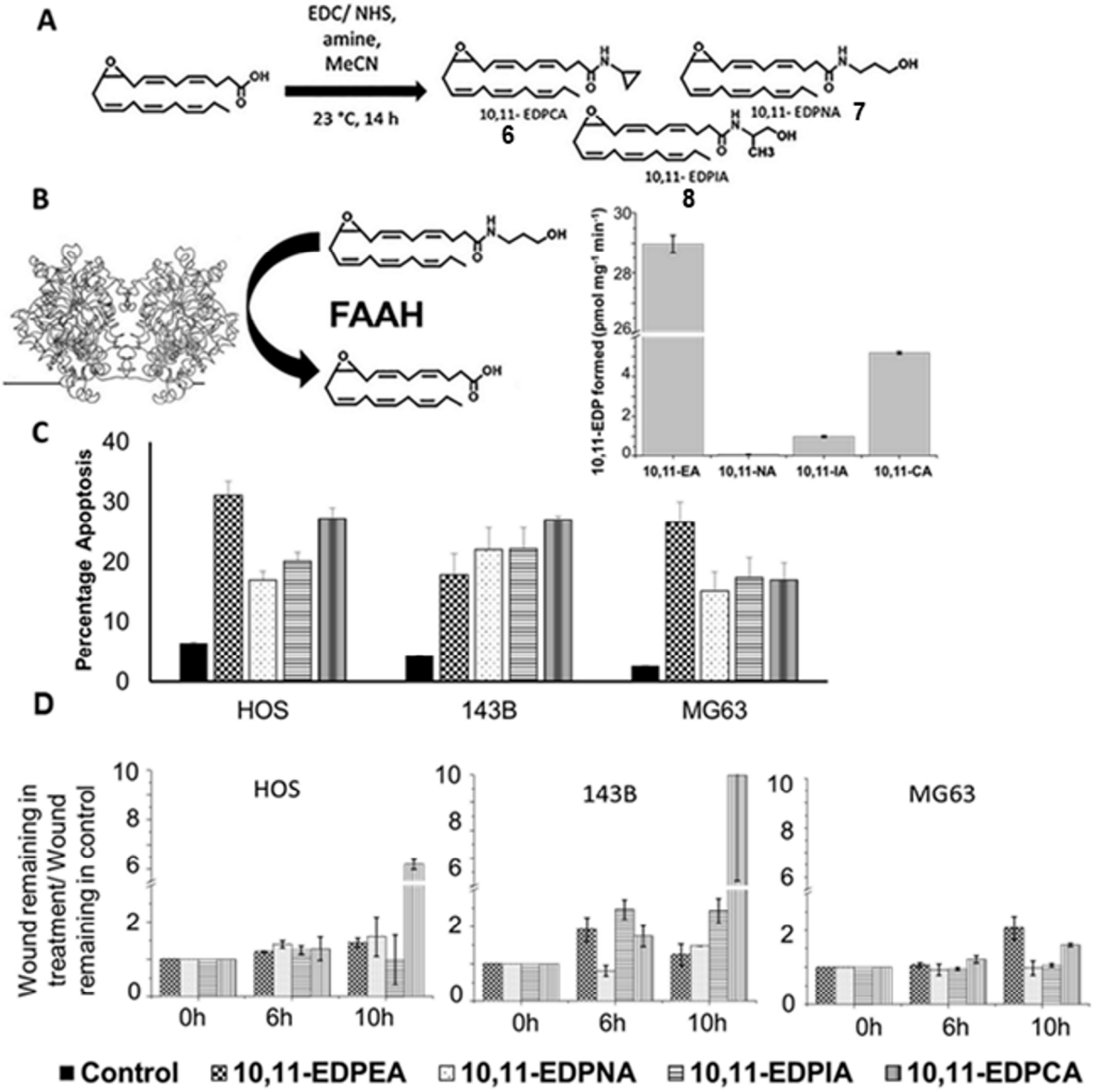

Figure 2: (A) Synthetic scheme for EDP-EA analogs (6-8). **(B)** Fatty Acid Amide Hydrolase (FAAH) dependent hydrolysis of amide derivatives. **(C)** Apoptotic potential of 10,11-EDP-EA (checkered), 10,11-EDP-NA (7) (dots), 10,11-EDP-IA (8) (horizontal stripes) and 10,11EDP-CA (6) (vertical stripes) as compared to control as measured by Annexin V apoptosis assay. **(D)** Anti-migratory properties of 10,11-EDP-EA, 10,11-EDP-NA, 10,11-EDP-IA and 10,11EDP-CA

as compared to control as measured by wound healing scratch assay on HOS, 143B and MG63 cell line

Cell cycle analysis of 10,11-EDP-EA and its analogs

The effects of 10,11-EDP-EA and its analogs were tested on cell cycle progression by treating cells with the compound for 24 hours, staining with propidium iodide and then analyzing with flow cytometry. Staining by PI reflects the percentage of cells in each stage of the cell cycle G1, S and G2. As seen in Table 1, in 143B cells there does not appear to be a significant effect on the cell cycle except a slight suppression in the S phase with 10,11-EDP-NA. However, with the HOS cell lines there is an increase in G1 phase with all compounds but a suppression in the S phase with all the compounds. Finally, with MG63 there is an increase in the G1 phase and suppression in S phase with the 10,11-EDP-IA.

Cell line	untreated	10,11-EDP-EA	10,11-EDP-NA	10,11-EDP-IA	10,11-EDP-CA
143B					
G1	56.2 ± 2.7	50.7 ± 2.03	52.2 ± 0.1	50.1 ± 0.03	54.2 ± 0.8
S	26.6 ± 0.4	28.9 ± 3.9	**24.0 ± 0.3***	41.8 ± 3.7	22.9 ± 0.3
G2	17.2 ± 2.3	21.1 ± 1.9	23.7 ± 0.4	8.1 ± 3.7	22.9 ± 0.4
HOS					
G1	47.8 ± 0.7	**67.2 ± 0.6**#**	**62.2 ± 0.4****	55.8 ± 5.0	**54.4 ± 1.4*#**
S	37.1 ± 1.6	**20.3 ± 0.9***	**20.7 ± 2.1***	**24.3 ± 1.4***	**30.5 ± 1.8#**
G2	15.1 ± 0.97	12.4 ± 0.3	17.1 ± 1.7	20.0 ± 3.7	**15.1 ± 0.4#**
MG63					
G1	62.9 ± 1.8	67.7 ± 2.2	63.5 ± 0.8	**76.7 ± 0.1***	59.6 ± 0.3
S	20.2 ± 1.8	17.9 ± 2.1	19.0 ± 0.4	**10.8 ± 0.3***	23.1 ± 0.4

G2	16.9 ± 0.01	**14.4 ± 0.2****	**17.5 ± 0.4#**	**12.5 ± 0.4**#**	**16.9 ± 0.1##**

Table 1: Table shows percentage of cells in each stage by cell cycle analysis using propidium iodide, of 10,11-EDP-EA, 10,11-EDP-NA, 10,11-EDP-IA and 10,11-EDP-CA as monitored by propidium iodide staining in all three cell lines. All experiments were done in triplicates. * $p<0.05$, ** $p<0.01$ as compared to untreated, # $p<0.05$, ## $p<0.01$ as compares to EA.

10,11-EDP-EA and its analogs prevent angiogenesis in HUVEC cells

Increased angiogenesis is one of the hallmarks of cancer. The development of neo-vascularization is key for the adequate supply of nutrients and oxygen to the site of metastasis. [40] Endothelial tube formation on matrix has been established as a cellular model for angiogenesis. [41] Endothelial HUVEC cells form a networks of tubes when plated on matrigel and the tube formation in presence and absence of treatment can be quantified as a measure of restricted angiogenic potential. Briefly, endothelial HUVEC cells were grown on matrix and treated with vehicle control, 0.5 μM compound or 1 μM compound. The tube formation was assessed by Image J analysis. As seen in figure 3a and b, 0.5 μM and 1 μM concentrations restrict tube formation significantly as compared to the vehicle control. It was also verified that 1 μM concentration of treatment did not reduce cell viability in HUVEC cells as seen in supplementary figure S5.

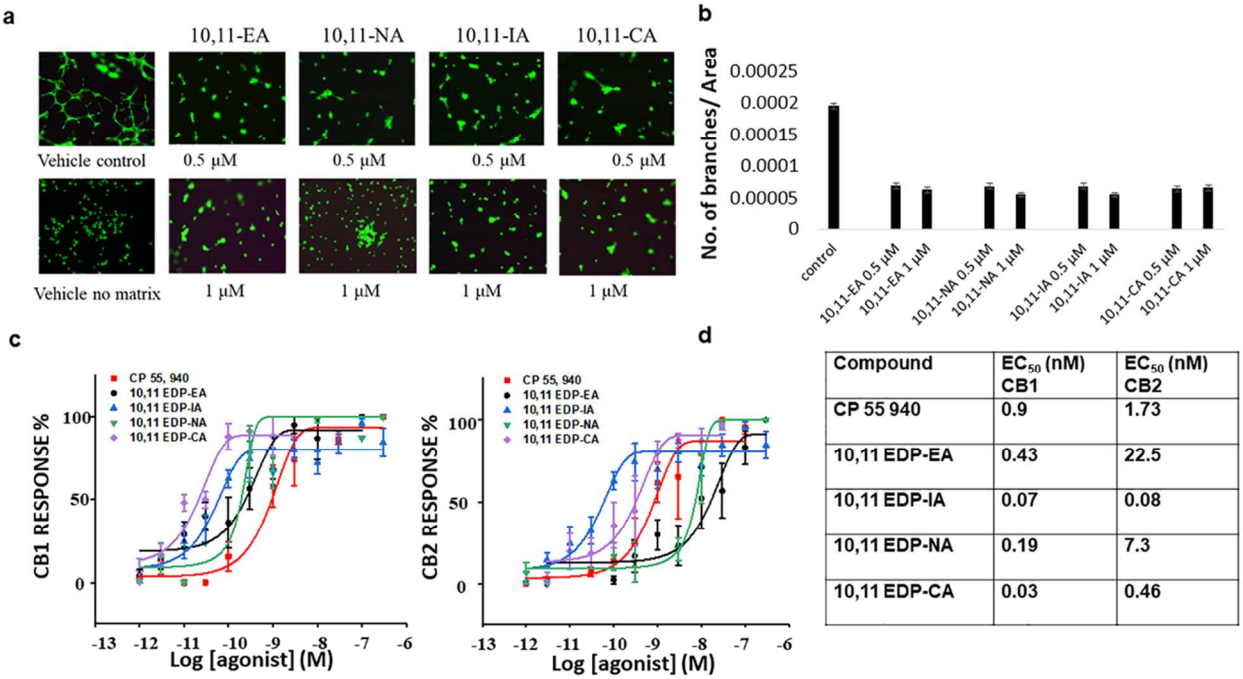

Compound	EC_{50} (nM) CB1	EC_{50} (nM) CB2
CP 55 940	0.9	1.73
10,11 EDP-EA	0.43	22.5
10,11 EDP-IA	0.07	0.08
10,11 EDP-NA	0.19	7.3
10,11 EDP-CA	0.03	0.46

Figure 3: (a) Restriction of tube formation in endothelial HUVEC cells on matrigel by 10,11-EDP-EA, 10,11-EDP-NA, 10,11-EDP-IA and 10,11EDP-CA at 0.5 µM and 1 µM. **(b)** Quantification of angiogenesis reduction by all amide derivatives as represented by number of branches per unit area. **(c)** Presto-Tango assay measurement of the activation of CB1 and CB2 by amide derivatives. **(d)** EC_{50} values of all amide derivatives with CB1 and CB2 by Presto-Tango assay.

Expression of CB1 and CB2 receptors in model cell lines

Literature evidence suggests that DHEA is an agonist of CB1 and CB2 receptors. [11] Therefore, we investigated whether the effect of DHEA is through CB1/ CB2 pathway mediated. Additionally, CB receptors have been shown to be overexpressed in various cancers including osteosarcoma. [42] We first determined the expression of CB1 and CB2 receptors in all three cell lines HOS, 143B and MG63 by qRT-PCR, which quantifies receptor expression by measuring

corresponding mRNA levels and comparing to a control marker like beta actin. As seen in figure S6, all three cell lines expressed both CB1 and CB2 in similar levels. Additionally, the expression of CB1 and CB2 was also significantly higher in 143B cells as compared to HOS cells ($p= 0.023$ and 0.021 for CB1 and CB2 respectively) as well as compared to MG63 cells ($p= 0.033$ and $p=0.027$ for CB1 and CB2 respectively).

Activation of CB1 and CB2 by 10,11-EDP-EA and its amide analogs

To investigate whether 10,11-EDP-EA and its amide modified analogs activated the cannabinoid receptors, a beta-arrestin recruitment PRESTO-Tango assay was performed in a dose-dependent manner for these compounds [43]. Presto-tango is an open-source resource developed by Roth group that allows interrogation of the human GPCRome by drugs and endogenous ligands. In this assay, upon ligand binding to a specific G protein-coupled receptor (GPCR), it triggers desensitization which mediated by the recruitment of protease-tagged arrestin proteins to the activated receptor. This protease-tagged arrestin then cleaves a protease site fused to the C-terminus of the GPCR that is being studies thus releasing a non-native transcription factor (TF). This TF regulates the transcription of a beta-lactamase reporter construct, which is measured upon addition of the luminogenic substrate. The activation of the reporter gene by the ligand/drug provides a quantifiable measurement of the degree of interaction between the target receptor and the protease-tagged arrestin partner. Briefly, HTLA cells transfected with either CB1 or CB2 were incubated with appropriate treatment and subsequently luminescence was measured as an indicator of receptor activation (Figure 3c and d). CP55940 was used as a control for this experiment and the EC_{50} values were observed to be 0.9 nM and 1.73 nM, which is in agreement with literature. [44] As observed in figure 3C, a dose response curve was obtained for 10,11-EDP-EA and its analogs. 10,11-EDP-EA has an EC_{50} value of 0.43 nM and 22.5 nM for

CB1 and CB2 respectively. This indicates that it shows higher activation of CB1 than CB2. A similar trend was observed for all 10,11-EDP-EA analogs. 10,11-EDP-NA had EC_{50} values of 0.19 nM and 7.3 nM respectively. 10,11-EDP-CA had EC_{50} values of 0.03 nM and 0.46 nM for CB1 and CB2, respectively. Finally, 10,11-EDP-IA showed the smallest differences in activation of CB1 and CB2 and showed EC_{50} values of 0.07 nM and 0.08 nM, respectively. Therefore, all amide analogs have increased activation of both CB1 and CB2 as compared to the parent compound 10,11-EDP-EA and all activate CB1 better than CB2. As observed in this data, 10,11-EDP-CA is the best activator of CB1. The cannabinoid receptor mediated reduction of cancer cell migration has been reported in literature, [19] and it can be hypothesized that 10,11-EDP-CA has increased anti-migratory potential due to increased activation of CB1.

Apoptotic effect of DHEA epoxides in the presence of CB1 and CB2 antagonists

As an initial investigation into the mechanism of action for these endocannabinoids, we assessed their apoptotic activity in the presence of CB1 and CB2 antagonists, rimonabant and AM 630 respectively. As seen from supplementary tables 2-4, rimonabant and AM 630 exhibit very limited apoptotic activity as compared to control. However, the blocking of CB1 and CB2 receptors has very limited effect on the apoptotic potential of the endocannabinoid epoxides. In HOS cell line (Table ST2), the decrease in apoptosis in presence of CB1 or CB2 antagonist or both is modest with all three regioisomers, indicating this is not the primary pathway of action by endocannabinoid epoxides. In 143B cells (Table ST3), when CB1 and CB2 antagonist were incubated with 7,8-EDP-EA, a slight increase in apoptotic activity with 14.6 ± 1.8% and 10.1 ± 1.4% respectively. A similar result was seen for 13,14-EDP-EA where the treatment plus CB1 antagonist showed 13.0 ± 3.6%. The treatment plus CB2 antagonist showed no difference in apoptosis as compared to treatment alone at 9.2 ± 0.8%. For 10,11-EDP-EA there was slight

suppression of apoptotic activity with both antagonists. The slight increase in apoptosis might be as a combinatorial effect of the treatment with the antagonist. Finally, as seen in table ST4, the effect of CB1 and CB2 antagonists on MG63 cells was similar to that observed in 143B cells. Alternatively, since the molecules have two different reactive centers, the epoxide as well as the amide, they likely act through two different receptor classes- the cannabinoid receptor and the unknown receptor for epoxy fatty acids. It is possible that the blocking of the CB1 or CB2 receptors shuttle the molecule to the second epoxide receptor pathway thereby increasing the apoptotic activity. Finally, 10,11-EDP-EA showed a decrease in apoptotic potential with CB1 and CB2 antagonist at 7.4 ± 2.2% and 10.9 ± 0.1% indicating that this molecule mainly goes through the CB1 and CB2 receptors.

DISCUSSION:

Lipid metabolites that are generated from omega-3 fatty acids such as DHA have been shown to exert anti-inflammatory, pro-resolving [4] and anti-tumorigenic effects through various mechanisms. [5 6 7] In one mechanism, DHA is converted to DHA epoxides (EDPs) by CYP epoxygenase that have shown to exhibit have anti-tumorigenic properties. Alternatively, DHA is converted to DHEA, an endocannabinoid that have shown anti-proliferative efficiency in prostate cancer cells. [11] Previously, we have shown that CYPs convert DHEA into DHEA epoxides (EDP-EA) that are dual functional molecules containing both ethanolamide and epoxide moiety [25] (Figure 1a) as both the endocannabinoid and epoxyeicosanoid pathway have been separately implicated in cancer [8, 9] and the terminal DHEA epoxide was shown to exhibit anti-inflammatory properties. [25] Herein we evaluated the anti-tumorigenic properties of all the different regioisomers of DHEA epoxides.

To ascertain the biological relevance of endocannabinoid epoxides in the tumor microenvironment, we induced tumors in mice and extracted total endocannabinoids from the lung metastasized tumor that showed that the DHEA epoxides were increased 20-80% depending on the regioisomers (Figure 1b) in the metastatic mice with osteosarcoma tumors as compared to the normal lungs. The bioactive lipids such as DHEA epoxides are generated by various cell types including immune cells. We hypothesize that the upregulation of cytochrome P450s in these tumor tissues and surrounding immune cells leads to the rapid synthesis of these DHEA epoxides that are anti-inflammatory,[25] anti-angiogenic, anti-metastatic and potentially pro-resolving. It has been shown before that pro-resolving mediators help in reduction of inflammation and modify the tumor micro environment.[45] We further show that the EDP-EAs show a reduction of migratory potential of the cancer cells and moderately increased apoptosis in osteosarcoma cell lines. We tested all the five epoxide regioisomers of EDP-EAs towards their ability to induce apoptosis in three human osteosarcoma cell lines- 143B, MG63 and HOS.

In all the three cell lines, the various regioisomers show an apoptotic effect and an anti-migratory effect and this is significantly higher than the parent molecules DHA and DHEA. However, this effect is differential among the various EDP-EA regioisomers. For instance, 10,11-EDP-EA emerges as the most potent regioisomer in reducing cell migration. Interestingly, this effect was mediated via the CB1 receptor as using a CB1 antagonist, the anti-migratory potential of 10,11-EDP-EA was significantly reduced (Supplementary figure 4).

Since 10,11-EDP-EA showed the greatest potency in our assays, we wanted to characterize the molecule and explore its therapeutic potential *in vivo*. However, EDP-EAs has two hydrolytically susceptible groups. The amide group is hydrolyzed by fatty acid amide hydrolase (FAAH) and the epoxide group is hydrolyzed by soluble epoxide hydrolases. Thus, we prepared synthetic

analogs that demonstrated similar apoptotic and migratory potentials (Figure 2c and 2d) as compared to parent 10,11-EDP-EA, but markedly reduced susceptibility to FAAH hydrolysis (Figure 2b).

The cannabinoid receptor mediated apoptosis has been characterized in literature and is thought to be mediated through ceramide synthesis. [46] Additionally, the CB1 mediated restriction of cell migration has also been studied. [47] In our studies, we show that while all endocannabinoid epoxides and their derivatives activate both cannabinoid receptors, their activity is not completely mediated through these receptors. Therefore, their activity could also be mediated through other receptors including the uncharacterized receptor for epoxy fatty acids, PPAR and TRPV. [48]

CONCLUSIONS

Taken all the findings together, we demonstrate a novel class of eCB epoxides and their stable derivatives exhibit anti-inflammatory, [30] anti-angiogenic, anti-tumorigenic and anti-migratory properties. These molecules particularly reduced the migratory ability of OS cells and therefore may be of greater therapeutic significance to prevent metastasis of tumor. By virtue of their ability to bind CB receptors, these molecules might also exhibit anti-nociceptive bone pain activities. As osteosarcoma and other cancers are accompanied by inflammation and pain, these molecules might aid in alleviating both conditions. These molecules are naturally occurring and their levels increase ~80% in osteosarcoma metastatic lungs, increasing their levels *in vivo* using FAAH and sEH dual inhibition will be effective adjuvant therapy for osteosarcoma. [49, 50]

EXPERIMENTAL SECTION

Materials: Annexin V/ PI kit was purchased from BD biosciences (556547). HUVEC cells were procured from Thermo Fisher (C0035C) and endothelial cell media was obtained from Lonza (EGM2 bullet kit CC-3162). Angiogenesis kit was purchased from Abcam (ab204726).

General synthesis of EDP-EAs (1-5): EDP-EA synthesis was performed in a two-step approach. First a non-specific epoxidation reaction with 50 mg of or DHA dissolved in 2 mL of dichloromethane (DCM) with 2 molar equivalents of metachloroperoxybenzoic acid (mCPBA) and was reacted for 1 h at room temperature. The reaction was stopped with an equal volume of 10% aqueous $NaHCO_3$ to remove mCPBA from the organic layer, and the aqueous layer was re-extracted thrice with equal volumes of DCM and the combined organic layer was dried *in vacuo*. Purification of regioisomers was achieved using normal-phase HPLC (NP-HPLC) using a Zorbax-NH_2 5 μm × 9.4 mm × 250 mm semipreparative column (Agilent, PN880952-208) with an isocratic gradient (hexane/isopropanol/acetic acid; 90:10:0.1) coupled to a HPLC system. For coeluting regioisomers of DHA epoxides (19,20-EDP and 13,14-EDP), the mixtures were further purified on the same system using reversed-phase HPLC (RP-HPLC), a Sun Fire Prep C18 5 μm × 19 mm × 50 mm column (PN 186002566; Waters), and a mobile system composed of solvent A (H2O/acetonitrile/acetic acid, 95:5:0.1), solvent B (H2O/acetonitrile/acetic acid, 5:95:0.1), and a linear gradient from 50% A to 0% A in 50 min.

In the second step, the coupling of the purified EDP regioisomer to ethanolamine was achieved by dissolving the epoxide in acetonitrile and incubating at 37 °C for 20 min with 1-ethyl-3-(3-dimethylaminopropyl)carbodiimide (EDC) and N-hydroxysuccinimide (NHS). Ethanolamine was subsequently added and the mixture was stirred overnight at room temperature. The resulting EDP-EA regioisomers were purified by RP-HPLC using a Sun Fire Prep C18 5 μm × 19 mm × 50 mm column (PN 186002566; Waters) and a mobile system composed of solvent A

(H20/acetonitrile/acetic acid 95:5:0.1) and solvent B (H20/acetonitrile/acetic acid 5:95:0.1) and a linear gradient from 50% A to 0% A in 50 minutes.

Isolation of endocannabinoids from tissue samples*:* K7M2 Experimental Metastasis Tumor Models of Osteosarcoma. All animal experimental procedures were reviewed and approved by the University of Illinois Institutional Animal Care and Use Committee (Protocol 15120). 1,000,000 K7M2 cells were prepared in HBSS and intravenously injected into the tail vein of 6−8 week old female BALB/c mice (day 0) in a 200 μL volume. After 14 days the mice were sacrificed and lung tissue was isolated, weighted and total endocannabinoids were extracted. The tissue was mechanically homogenized on ice with a BioHomogenizer (BioSpec) in a 1:1 ratio with PBS supplemented with sEH inhibitor 12-(3-adamantan-1-yl-ureido)-dodecanoic acid (AUDA) (Cayman Chemical) (30 μm) and FAAH inhibitor PMSF (1 mM) till a homogenous slurry was formed. 1 g of tissue was homogenized with 40 mL of ethyl acetate/hexane (9:1) using a BioHomogenizer (BioSpec) at room temperature and then was sonicated for 1 min. The resulting solution was washed with a 30% volume of water and centrifuged for the layers to separate. The organic layer was removed, and the aqueous layer was extracted with an equal volume of ethyl acetate/hexane (9:1) twice. The total organic layer was concentrated *in vacuo* using a Buchi 120 rotary evaporator and was reconstituted in 1 mL of chloroform. The metabolites of interest were isolated by solid-phase extraction (SPE) using a 1-mL silica gel column (no. 214477; Sigma). The reconstituted samples were added to the silica column and washed in three column volumes of chloroform, and consequently eluted with four column volumes of methanol/chloroform (1:9). The eluent was dried, and samples were reconstituted in ethanol for analysis via LC-MS/MS.

Liquid chromatography mass spectrometry analysis. The LC separation was performed on an Agilent Eclipse XDB-C18 (4.6 x 150mm, 5μm) with mobile phase A (0.1% formic acid in water) and mobile phase B (0.1% formic acid in acetonitrile). The flow rate was 0.4 mL/min. The linear gradient was as follows: 0-2min, 90%A; 8min, 55%A; 13-25min, 40%A; 30min, 30%A; 35min, 25%A; 40-47min, 20%A; 47.5-54min, 90%A. The autosampler was set at 5°C. The injection volume was 10 μL. Positive mass spectra were acquired with the ion spray voltage of 5500 V under electrospray ionization (ESI). The source temperature was 450°C. The curtain gas, ion source gas 1, and ion source gas 2 were 32 psi, 60 psi, and 60 psi, respectively. Multiple reaction monitoring (MRM) was used for quantitation: 19,20-EDP-EA and 7,8-EDP-EA m/z 388.1 → m/z 62.1; 16,17-EDP-EA, 13,14-EDP-EA, and 10,11-EDP-EA m/z 388.1 → m/z 370.1; DHEA 372.4 à m/z 62.1; Anandamide m/z 348.3 à m/z 62.1. Internal standards were monitored at: m/z 376.4 → m/z 66.1 for DHEA-d4.

Cell culture: Human cell lines HOS, MG63 and 143B were cultured in DMEM (Gibco, Invitrogen, Carlsbad, CA, USA) supplemented with 10% fetal bovine serum (FBS) and 1mg ml^{-1} penicillin–streptomycin (Gibco, Invitrogen) at 37 °C and 5% CO_2 in a humidified incubator.

Cell titer blue assay: 20,000 cells were plated per well in 96 well plates and allowed to adhere overnight. In the morning, the cell media was aspirated and replaced with fresh 100 μL of cell media and incubated with compound or DMSO vehicle control (1 μL) and allowed to incubate at 37 °C and 5% CO2 in a humidified incubator for 4 hours. 20 μL of cell titer blue reagent was added and the plate was incubated for 1 hour before the fluorescence was read using a plate reader with excitation at 534 nm and emission at 590 nm.

Annexin V assay*:* Annexin V kit from BD biosciences) was used. Briefly, cells were scraped and collected with the dead cells. They were washed with ice cold 2X PBS twice and

resuspended in 1X binding buffer and incubated with annexin V-FITC and propidium iodide for 15 mins, followed by flow cytometry by BD Accuri C6 instrument. Annexin V/PI assay was performed as per manufacturer's instructions. Briefly, cells were trypsinized and collected for analysis. Dead cells in the media were collected for testing along with the rest of the sample. The total cell sample was washed twice with cold PBS and then resuspended in 100 μL of binding buffer. 5 μL of each annexin V and PI were added and the cells were vortexed and incubated in the dark for 15 mins. The cells were then diluted with 400 μL of binding buffer and analyzed by BD Accuri flow cytometer within an hour. The treated samples were compared with negative and positive stained samples both with vehicle control.

Wound healing assay: Cells were grown to a confluent monolayer in 12 well plates and a scratch was made across the center of the plate with a pipette tip and images were taken. The media was replaced with fresh media and treatment or vehicle control was added to the wells. The cells were maintained at 37 °C and 5% CO_2 in a humidified incubator and images were taken every two hours. The images were processed using ImageJ via the wound healing plugin and normalized to 100% area at time 0.

General synthesis of amine EDP-EAs and analogs (1-8): To a solution of epoxide in acetonitrile, a solution of 1-ethyl-3-(3-dimethylaminopropyl) carbodiimide (EDC) (10 mg/mL in acetonitrile) and N-hydroxysuccinimide (NHS) (10 mg/mL in acetonitrile) in the ratio of (1:50:50) was added and incubated at 37 °C for 20 mins. To this we added the amine solution (2 mg mL^{-1} in acetonitrile) in the ratio of 1:50 with epoxide and this was stirred at room temperature overnight. The acetonitrile was removed under reduced pressure. The sample was reconstituted in ethanol and purified via HPLC. Purification of 10,11-EDP derivatives was performed using a reversed phase HPLC (RP-HPLC), Sun Fire Prep C18 5 μm 19 x 50 mm

(Waters, PN 186002566) and a mobile system composed of solvent A (H20/acetonitrile/acetic acid 95:5:0.1) and solvent B (H20/acetonitrile/acetic acid 5:95:0.1) and a linear gradient from 50% A to 0% A in 50 minutes. Compounds 1-5 have been previously synthesized and characterized.[30] HR-ESI and ^{1}H- NMR characterization performed is detailed below and ^{1}H NMR spectra are shown in Supplementary figures 7-10. All compounds showed >95% purity by ^{1}H-NMR analysis.

(4Z,7Z)-N-(2-hydroxyethyl)-9-(3-((2Z,5Z,8Z)-undeca-2,5,8-trien-1-yl)oxiran-2-yl)nona-4,7-dienamide Or 10,11- EDP-EA (2) : Synthesis was performed as mentioned in previous section using 10,11-EDP and ethanolamine. HR-ESI-MS (m/z) 387.2821, $[M+H]^+$ calculated ($C_{24}H_{38}NO_3$): 387.28

^{1}H NMR: 5.58-5.27 (m, 10H), 3.77-3.62 (m, 3H), 3.45-3.32 (m, 2H), 3.29- 3.22 (t, 2H), 3.21-3.15 (d, 1H), 3.03-2.94 (m, 2H), 2.88-2.75 (m, 4H), 2.75-2.65 (t, 1H), 2.32-2.22 (m, 5H), 1.15-1.09 (t, 3H), 1.00-0.94 (t, 3H)

(4Z,7Z)-N-cyclopropyl-9-(3-((2Z,5Z,8Z)-undeca-2,5,8-trien-1-yl)oxiran-2-yl)nona-4,7-dienamide or 10,11-EDP-CA (6*): Synthesis was performed as mentioned in previous section using 10,11-EDP and cyclopropylamine. HR-ESI-MS (m/z) found: 384.2910; $[M+H]^+$ calculated $C_{25}H_{38}NO_3$: 383.58

^{1}H NMR: 5.57-5.22 (m, 10H), 3.30-3.24 (t, 2H), 3.24- 3.14 (q, 2H), 2.99-2.93 (m, 1H), 2.87-2.77 (m, 6H), 2.73-2.66 (m, 1H), 2.42- 2.36 (m, 3H), 2.20-2.14 (t, 2H), 2.12-2.05 (t, 2H), 1.87-79 (t, 2H), 1.00-0.92 (t, 3H), 0.88-0.84 (t, 3H)

(4Z,7Z)-N-(3-hydroxypropyl)-9-(3-((2Z,5Z,8Z)-undeca-2,5,8-trien-1-yl)oxiran-2-yl)nona-4,7-dienamide or 10,11-EDP-NA (7) : Synthesis was performed as mentioned in previous

section using 10,11-EDP and 3-amino-1-propanol. HR-ESI-MS (m/z) found [M+Na]: 424.2891; $[M+H]^+$ calculated $C_{25}H_{40}NO_3$: 401.29

^{1}H NMR: 5.59-5.27 (m, 10H), 3.88-2.79 (t, 1H), 3.75-3.69 (q, 2H), 3.66-3.59 (m, 2H), 3.45-3.38 (m, 2H), 3.28-2.23 (t, 1H), 3.22-3.15 (m, 1H),3.04-2.95 (m, 2 H), 2.91- 2.72 (m, 4H), 2.67- 2.63 (s, 1H), 2.62-2.58 (t, 1H), 2.48-2.40 (m, 1H), 2.31-2.21 (m, 2H), 1.28-1.22 (m, 4H), 1.15-1.10 (t, 2H), 1.00-0.95 (t, 2H)

(4Z,7Z)-N-(1-hydroxypropan-2-yl)-9-(3-((2Z,5Z,8Z)-undeca-2,5,8-trien-1-yl)oxiran-2-yl)nona-4,7-dienamide or 10,11-EDP-IA (8): Synthesis was performed as mentioned in previous section using 10,11-EDP and R-(-)2-amino-1-propanol. HR-ESI-MS (m/z) found: 402.2901; $[M+H]^+$ calculated $C_{25}H_{40}NO_3$: 401.29

^{1}H NMR: 5.57-5.26 (m, 10H), 4.16-3.98 (m, 3H), 3.71-3.57 (m, 2H), 3.57-3.44 (m, 3H), 3.09-2.98 (m, 1H), 2.89-2.75 (m, 4H), 2.46-2.33 (m, 4 H), 2.22-2.21 (m, 3H), 2.11-1.99 (m, 2H), 0.99-0.94 (t, 3H), 0.89-0.85 (t, 3H).

Cell cycle analysis: 80% confluent cells in a 12 well plate were treated for 24 hours with appropriate treatment and harvested. Cells were washed twice with PBS and fixed with 70% ethanol in ice for 30 mins by vortexing to prevent clumping. The cells were washed twice with PBS and were incubated with a 50 µL of a 100 µg mL^{-1} RNase solution for 30 mins on ice followed by addition of 200 µL of 50 µg mL^{-1} propidium iodide solution before analysis by BD LSR II flow cytometer and analyzed by FCS software.

FAAH hydrolysis: The preparation of pig forebrain membranes was achieved using dounce homogenization in buffer (50 mM Tris pH 7.4, 1 mM EDTA and 3 mM $MgCl_2$) and membrane

pelleting as previously described. [39] Incubations contained 5 µg forebrain protein in a 0.5 mL reaction containing 50 mM Tris (pH 7.4), 1 mM EDTA, 3 mM $MgCl_2$, and amide at 20 µM. At 40 min reactions were quenched with methanol containing 1 mM PMSF and centrifuged to pellet protein (10,000 g x 10 min). The supernatant was collected and analyzed via LC-MS/MS as outlined below.

Analysis of 10,11-EDP by LC-MS/MS: Analyses were performed using the 5500 QTRAP LC/MS/MS system (AB Sciex, Foster City, CA) in Metabolomics Lab of Roy J. Carver Biotechnology Center, University of Illinois at Urbana-Champaign. The 1200 series HPLC system (Agilent Technologies, Santa Clara, CA) includes a degasser, an autosampler, and a binary pump, and this system was used to separate the metabolites. LC separation was performed on an Agilent Eclipse XDB-C18 (4.6 x 150mm, 5µm) with mobile phase A (0.1% formic acid in 20 water) and mobile phase B (0.1% formic acid in acetonitrile) at a flow rate was 0.4 mL/min. The linear gradient was as follows: 0-2min, 90%A; 8min, 55%A; 13-25min, 40%A; 30min, 30%A; 35min, 25%A; 40min, 20%A; 45-47min, 15%A; 48-54min, 90%A. The autosampler was set at 5°C. The injection volume was 10 µL. Negative mass spectra were acquired with the ion spray voltage of -4500 V under electrospray ionization (ESI). The source temperature was 450 °C. The curtain gas, ion source gas 1, and ion source gas 2 were 32 psi, 50 psi, and 55 psi, respectively. Multiple reaction monitoring (MRM) was used for quantitation: 10,11-EDP m/z 343.0.

Presto-Tango β-arrestin recruitment assay: The PRESTO-Tango β-arrestin recruitment assay. The Presto-Tango β-arrestin recruitment assay was used for the measurement of CB1 (or CNR1) and CB2 (CNR2) GPCR activation as previously described (4). HTLA cells, CNR1 (Addgene #66254) and CNR2 (Addgene #66255) plasmids were a generous gift from the Roth Lab (UNC

Chapel Hill). HTLA cells were maintained in DMEM with 10% FBS containing 2 μg mL^{-1} of puromycin and 100 μg/mL of hygromycin B at 37 °C in a 5% CO_2 humidified air atmosphere and grown to 80-90% confluency. Cells were then seeded at 20,000 cells per 100 μL into a poly-L-lysine coated 96-well plate. After 18-24 hrs, cells were transfected with CNR1 or CNR2 plasmids (0.1 μg per well) using Calfectin (0.4 μL) as the transfection reagent in a 4:1 reagent to plasmid ratio (final well vol. 110 μL). Transfection media was replaced after 12-18 hours with fresh serum-media and maintained for 36-48 hours. On the day of the assay, serum-media was replaced with 100 μL media containing 1% dialyzed FBS for 4 hours, then compound was further diluted with media containing 1% dialyzed FBS and was added in a log dose manner (final well vol. 200 μL) and incubated for 8-14 hours. For epoxygenated metabolites, serum-media was replaced with 100 μL media containing 1% dialyzed FBS and 1 μM AUDA for 30 min, then compound was further diluted with media containing 1% dialyzed FBS and was added in a log dose manner (final well vol. 200 μL including the media with AUDA) and incubated for 8-14 hours. The following day, media was removed and 40 μL of diluted Bright-Glo solution (Promega, Madison, WI) was added to each well and incubated in the dark for 20min at room temperature before luminescence recordings. Relative luminescence units (RLU) values were normalized to % receptor response, plotted as a function of compound concentration and analyzed using "DoseResp" in OriginPro.

Angiogenesis Assay: Angiogenesis in endothelial HUVEC cells was measured using abcam angiogenesis kit (ab204726). Briefly, HUVEC cells at passage 2 (p=2) were grown to 80% confluency. The matrigel provided was thawed overnight and 50 μL was put into each well of a 96 well plate that had been chilled overnight in a -20 °C freezer. The plate was rocked slightly and then allowed to incubate at 37 °C for 1 hour. 15,000 HUVEC cells were then plated into the

wells and were treated with vehicle control or 0.5 μM or 1 μM compound. A no matrix control and a control with vinblastine (inhibitor of angiogenesis) was also performed. All wells were performed in duplicates. The plates were then incubated for 5 hours at 37 °C. The incubation medium was removed and cells were washed with 100 μL of wash buffer. 100 μL of staining dye was added to each well and incubated for 30 mins at 37 °C. The wells were imaged using a fluorescent microscope and analyzed using ImageJ with Angiogenesis Analyzer Plugin.

ACKNOWLEDGMENTS

Funding Sources. Partially supported by American Heart Association Scientist Development Grant 15SDG25760064 (A.D.), National Institutes of Health (NIH) Grant R01 GM1155884 (A.D.) and NIH Grant R03 DA042365. The authors greatly appreciate the contributions of Dr. Z. Li at the Metabolomics Laboratory of Roy J. Carver Biotechnology Center, University of Illinois at Urbana-Champaign. We thank Ms. H. Pondenis, Dr. K.Wycislo and Ms. Nicole Sidebotham for helpful discussion.

AUTHOR CONTRIBUTIONS

AD and JR conceived the paper, JR, JEW, IH performed the experiments, AD and JR analyzed the data, JEW performed PRESTO-Tango assay, IH contributed to compounds synthesis. AD, JR, TF wrote and edited the paper.

COMPETING FINANCIAL INTERESTS

The authors declare no competing financial interests.

SUPPORTING INFORMATION: All supporting information has been included in attached supplementary information file.

- Endocannbinoid fold change in normal vs metastatic lungs, full range CTB assay, apoptosis assay with parent fatty acids, 7,8-, 10,11- and 13,14-EDP-EA in presence of CB1 and CB2 inhibitors in all three cell lines, scratch assay in 143B cells, CTB assay with HUVEC cells, qRT-PCR for CB1 and CB2, NMRs of 10,11-EDP-NA, 10,11-EDP-

IA and 10,11-EDP-CA, scratch assay of 10,11-EDP-CA in 143B cells with CB1 and CB2 antagonists, Angiogenesis assay with 10,11-EDP-EA and its analogs in HUVEC cells.

- SMILES strings and the corresponding biological data (CSV file)

CORRESPONDING AUTHOR Aditi Das, aditidas@illinois.edu

ABBREVIATIONS: CYP: cytochrome P450; AA: arachidonic acid; EPA: eicosapentaenoic acid; EEQ: epoxyeicosatrienoic acid; EEQ-EA: epoxyeicosatrienoic-ethanolamide; DHA: docosahexaenic acid; EDP: epoxydocosapentaenoic acid; EDP-EA: epoxydocosapentaenoic-ethanolamide; sEH: soluble epoxide hydrolase; FAAH: fatty acid amide hydrolase; LC-MS/MS: liquid chromatography mass spectrometry-mass spectrometry

REFERENCES:

1. Mantovani, A.; Allavena, P.; Sica, A.; Balkwill, F. Cancer-related inflammation. *Nature* **2008,** 454, 436-44.
2. Sica, A.; Allavena, P.; Mantovani, A. Cancer related inflammation: the macrophage connection. *Cancer Lett* **2008,** 267, 204-15.
3. Yu, H.; Pardoll, D.; Jove, R. STATs in cancer inflammation and immunity: a leading role for STAT3. *Nat Rev Cancer* **2009,** 9, 798-809.
4. Jaudszus, A.; Gruen, M.; Watzl, B.; Ness, C.; Roth, A.; Lochner, A.; Barz, D.; Gabriel, H.; Rothe, M.; Jahreis, G. Evaluation of suppressive and pro-resolving effects of EPA and DHA in human primary monocytes and T-helper cells. *J Lipid Res* **2013,** 54, 923-35.
5. Laviano, A.; Rianda, S.; Molfino, A.; Rossi Fanelli, F. Omega-3 fatty acids in cancer. *Curr Opin Clin Nutr Metab Care* **2013,** 16, 156-61.
6. Rose, D. P.; Connolly, J. M. Omega-3 fatty acids as cancer chemopreventive agents. *Pharmacology & Therapeutics* **1999,** 83, 217-244.
7. D'Eliseo, D.; Velotti, F. Omega-3 Fatty Acids and Cancer Cell Cytotoxicity: Implications for Multi-Targeted Cancer Therapy. *J Clin Med* **2016,** 5.
8. Cui, P. H.; Petrovic, N.; Murray, M. The omega-3 epoxide of eicosapentaenoic acid inhibits endothelial cell proliferation by p38 MAP kinase activation and cyclin D1/CDK4 down-regulation. *Br J Pharmacol* **2011,** 162, 1143-55.
9. Zhang, G.; Panigrahy, D.; Mahakian, L. M.; Yang, J.; Liu, J. Y.; Stephen Lee, K. S.; Wettersten, H. I.; Ulu, A.; Hu, X.; Tam, S.; Hwang, S. H.; Ingham, E. S.; Kieran, M. W.; Weiss, R. H.; Ferrara, K. W.; Hammock, B. D. Epoxy metabolites of docosahexaenoic acid (DHA) inhibit angiogenesis, tumor growth, and metastasis. *Proc Natl Acad Sci U S A* **2013,** 110, 6530-5.
10. Brown, I.; Cascio, M. G.; Rotondo, D.; Pertwee, R. G.; Heys, S. D.; Wahle, K. W. Cannabinoids and omega-3/6 endocannabinoids as cell death and anticancer modulators. *Prog Lipid Res* **2013,** 52, 80-109.

11. Brown, I.; Cascio, M. G.; Wahle, K. W.; Smoum, R.; Mechoulam, R.; Ross, R. A.; Pertwee, R. G.; Heys, S. D. Cannabinoid receptor-dependent and -independent anti-proliferative effects of omega-3 ethanolamides in androgen receptor-positive and -negative prostate cancer cell lines. *Carcinogenesis* **2010,** 31, 1584-91.
12. Di Marzo, V. Endocannabinoids: synthesis and degradation. *Rev Physiol Biochem Pharmacol* **2008,** 160, 1-24.
13. Skaper, S. D.; Di Marzo, V. Endocannabinoids in nervous system health and disease: the big picture in a nutshell. *Philos Trans R Soc Lond B Biol Sci* **2012,** 367, 3193-200.
14. Fonseca, B. M.; Costa, M. A.; Almada, M.; Correia-da-Silva, G.; Teixeira, N. A. Endogenous cannabinoids revisited: a biochemistry perspective. *Prostaglandins Other Lipid Mediat* **2013,** 102-103, 13-30.
15. Ashton, J. C.; Glass, M. The cannabinoid CB2 receptor as a target for inflammation-dependent neurodegeneration. *Current Neuropharmacology* **2007,** 5, 73-80.
16. Onaivi, E. S. Cannabinoid receptors in brain: pharmacogenetics, neuropharmacology, neurotoxicology, and potential therapeutic applications. *Int Rev Neurobiol* **2009,** 88, 335-69.
17. Vara, D.; Salazar, M.; Olea-Herrero, N.; Guzman, M.; Velasco, G.; Diaz-Laviada, I. Anti-tumoral action of cannabinoids on hepatocellular carcinoma: role of AMPK-dependent activation of autophagy. *Cell Death Differ* **2011,** 18, 1099-111.
18. Ladin, D. A.; Soliman, E.; Griffin, L.; Van Dross, R. Preclinical and Clinical Assessment of Cannabinoids as Anti-Cancer Agents. *Frontiers in Pharmacology* **2016,** 7.
19. Guindon, J.; Hohmann, A. G. The endocannabinoid system and cancer: therapeutic implication. *Br J Pharmacol* **2011,** 163, 1447-63.
20. Schwarz, R.; Ramer, R.; Hinz, B. Targeting the endocannabinoid system as a potential anticancer approach. *Drug Metab Rev* **2018,** 50, 26-53.
21. Hsu, S. S.; Huang, C. J.; Cheng, H. H.; Chou, C. T.; Lee, H. Y.; Wang, J. L.; Chen, I. S.; Liu, S. I.; Lu, Y. C.; Chang, H. T.; Huang, J. K.; Chen, J. S.; Jan, C. R. Anandamide-induced Ca2+ elevation leading to p38 MAPK phosphorylation and subsequent cell death via apoptosis in human osteosarcoma cells. *Toxicology* **2007,** 231, 21-9.
22. De Petrocellis, L.; Melck, D.; Palmisano, A.; Bisogno, T.; Laezza, C.; Bifulco, M.; Di Marzo, V. The endogenous cannabinoid anandamide inhibits human breast cancer cell proliferation. *Proc Natl Acad Sci U S A* **1998,** 95, 8375-80.
23. Patsos, H. A.; Hicks, D. J.; Dobson, R. R.; Greenhough, A.; Woodman, N.; Lane, J. D.; Williams, A. C.; Paraskeva, C. The endogenous cannabinoid, anandamide, induces cell death in colorectal carcinoma cells: a possible role for cyclooxygenase 2. *Gut* **2005,** 54, 1741-50.
24. Nithipatikom, K.; Endsley, M. P.; Isbell, M. A.; Falck, J. R.; Iwamoto, Y.; Hillard, C. J.; Campbell, W. B. 2-arachidonoylglycerol: a novel inhibitor of androgen-independent prostate cancer cell invasion. *Cancer Res* **2004,** 64, 8826-30.
25. McDougle, D. R.; Watson, J. E.; Abdeen, A. A.; Adili, R.; Caputo, M. P.; Krapf, J. E.; Johnson, R. W.; Kilian, K. A.; Holinstat, M.; Das, A. Anti-inflammatory omega-3 endocannabinoid epoxides. *Proc Natl Acad Sci U S A* **2017**.
26. Niu, F.; Zhao, S.; Xu, C. Y.; Sha, H.; Bi, G. B.; Chen, L.; Ye, L.; Gong, P.; Nie, T. H. Potentiation of the antitumor activity of adriamycin against osteosarcoma by cannabinoid WIN-55,212-2. *Oncol Lett* **2015,** 10, 2415-2421.
27. Hald, A.; Ding, M.; Egerod, K.; Hansen, R. R.; Konradsen, D.; Jorgensen, S. G.; Atalay, B.; Nasser, A.; Bjerrum, O. J.; Heegaard, A. M. Differential effects of repeated low dose

treatment with the cannabinoid agonist WIN 55,212-2 in experimental models of bone cancer pain and neuropathic pain. *Pharmacol Biochem Behav* **2008,** 91, 38-46.
28. Lozano-Ondoua, A. N.; Wright, C.; Vardanyan, A.; King, T.; Largent-Milnes, T. M.; Nelson, M.; Jimenez-Andrade, J. M.; Mantyh, P. W.; Vanderah, T. W. A cannabinoid 2 receptor agonist attenuates bone cancer-induced pain and bone loss. *Life Sci* **2010,** 86, 646-53.
29. Luu, H. H.; Kang, Q.; Park, J. K.; Si, W.; Luo, Q.; Jiang, W.; Yin, H.; Montag, A. G.; Simon, M. A.; Peabody, T. D.; Haydon, R. C.; Rinker-Schaeffer, C. W.; He, T. C. An orthotopic model of human osteosarcoma growth and spontaneous pulmonary metastasis. *Clin Exp Metastasis* **2005,** 22, 319-29.
30. McDougle, D. R.; Watson, J. E.; Abdeen, A. A.; Adili, R.; Caputo, M. P.; Krapf, J. E.; Johnson, R. W.; Kilian, K. A.; Holinstat, M.; Das, A. Anti-inflammatory omega-3 endocannabinoid epoxides. *Proc Natl Acad Sci U S A* **2017,** 114, E6034-E6043.
31. Liang, C. C.; Park, A. Y.; Guan, J. L. In vitro scratch assay: a convenient and inexpensive method for analysis of cell migration in vitro. *Nat Protoc* **2007,** 2, 329-33.
32. Boyd, S. T.; Fremming, B. A. Rimonabant--a selective CB1 antagonist. *Ann Pharmacother* **2005,** 39, 684-90.
33. Abadji, V.; Lin, S. Y.; Taha, G.; Griffin, G.; Stevenson, L. A.; Pertwee, R. G.; Makriyannis, A. (R)-Methanandamide - a Chiral Novel Anandamide Possessing Higher Potency and Metabolic Stability. *Journal of Medicinal Chemistry* **1994,** 37, 1889-1893.
34. Jarrahian, A.; Manna, S.; Edgemond, W. S.; Campbell, W. B.; Hillard, C. J. Structure-activity relationships among N-arachidonylethanolamine (anandamide) head group analogues for the anandamide transporter. *Journal of Neurochemistry* **2000,** 74, 2597-2606.
35. Pinto, J. C.; Potie, F.; Rice, K. C.; Boring, D.; Johnson, M. R.; Evans, D. M.; Wilken, G. H.; Cantrell, C. H.; Howlett, A. C. Cannabinoid Receptor-Binding and Agonist Activity of Amides and Esters of Arachidonic-Acid. *Molecular Pharmacology* **1994,** 46, 516-522.
36. Sheskin, T.; Hanus, L.; Slager, J.; Vogel, Z.; Mechoulam, R. Structural requirements for binding of anandamide-type compounds to the brain cannabinoid receptor. *Journal of Medicinal Chemistry* **1997,** 40, 659-667.
37. Giang, D. K.; Cravatt, B. F. Molecular characterization of human and mouse fatty acid amide hydrolases. *Proceedings of the National Academy of Sciences of the United States of America* **1997,** 94, 2238-2242.
38. Goparaju, S. K.; Kurahashi, Y.; Suzuki, H.; Ueda, N.; Yamamoto, S. Anandamide amidohydrolase of porcine brain: cDNA cloning, functional expression and site-directed mutagenesis. *Biochimica Et Biophysica Acta-Molecular and Cell Biology of Lipids* **1999,** 1441, 77-84.
39. Hillard, C. J.; Wilkison, D. M.; Edgemond, W. S.; Campbell, W. B. Characterization of the kinetics and distribution of N-arachidonylethanolamine (anandamide) hydrolysis by rat brain. *Biochim Biophys Acta* **1995,** 1257, 249-56.
40. Nishida, N.; Yano, H.; Nishida, T.; Kamura, T.; Kojiro, M. Angiogenesis in cancer. *Vasc Health Risk Manag* **2006,** 2, 213-9.
41. Arnaoutova, I.; Kleinman, H. K. In vitro angiogenesis: endothelial cell tube formation on gelled basement membrane extract. *Nat Protoc* **2010,** 5, 628-35.
42. Chakravarti, B.; Ravi, J.; Ganju, R. K. Cannabinoids as therapeutic agents in cancer: current status and future implications. *Oncotarget* **2014,** 5, 5852-5872.

43. Kroeze, W. K.; Sassano, M. F.; Huang, X. P.; Lansu, K.; McCorvy, J. D.; Giguere, P. M.; Sciaky, N.; Roth, B. L. PRESTO-Tango as an open-source resource for interrogation of the druggable human GPCRome. *Nat Struct Mol Biol* **2015,** 22, 362-9.
44. Yin, H.; Chu, A.; Li, W.; Wang, B.; Shelton, F.; Otero, F.; Nguyen, D. G.; Caldwell, J. S.; Chen, Y. A. Lipid G protein-coupled receptor ligand identification using beta-arrestin PathHunter assay. *J Biol Chem* **2009,** 284, 12328-38.
45. Zhang, Q.; Zhu, B.; Li, Y. Resolution of Cancer-Promoting Inflammation: A New Approach for Anticancer Therapy. *Front Immunol* **2017,** 8, 71.
46. Cianchi, F.; Papucci, L.; Schiavone, N.; Lulli, M.; Magnelli, L.; Vinci, M. C.; Messerini, L.; Manera, C.; Ronconi, E.; Romagnani, P.; Donnini, M.; Perigli, G.; Trallori, G.; Tanganelli, E.; Capaccioli, S.; Masini, E. Cannabinoid Receptor Activation Induces Apoptosis through Tumor Necrosis Factor alpha - Mediated Ceramide De novo Synthesis in Colon Cancer Cells. *Clinical Cancer Research* **2008,** 14, 7691-7700.
47. Song, Z. H.; Zhong, M. CB1 cannabinoid receptor-mediated cell migration. *Journal of Pharmacology and Experimental Therapeutics* **2000,** 294, 204-209.
48. Di Marzo, V.; De Petrocellis, L. Why do cannabinoid receptors have more than one endogenous ligand? *Philosophical Transactions of the Royal Society B-Biological Sciences* **2012,** 367, 3216-3228.
49. Zhang, G.; Panigrahy, D.; Hwang, S. H.; Yang, J.; Mahakian, L. M.; Wettersten, H. I.; Liu, J. Y.; Wang, Y.; Ingham, E. S.; Tam, S.; Kieran, M. W.; Weiss, R. H.; Ferrara, K. W.; Hammock, B. D. Dual inhibition of cyclooxygenase-2 and soluble epoxide hydrolase synergistically suppresses primary tumor growth and metastasis. *Proc Natl Acad Sci U S A* **2014,** 111, 11127-32.
50. Winkler, K.; Ramer, R.; Dithmer, S.; Ivanov, I.; Merkord, J.; Hinz, B. Fatty acid amide hydrolase inhibitors confer anti-invasive and antimetastatic effects on lung cancer cells. *Oncotarget* **2016,** 7, 15047-64.

Table of Contents graphic

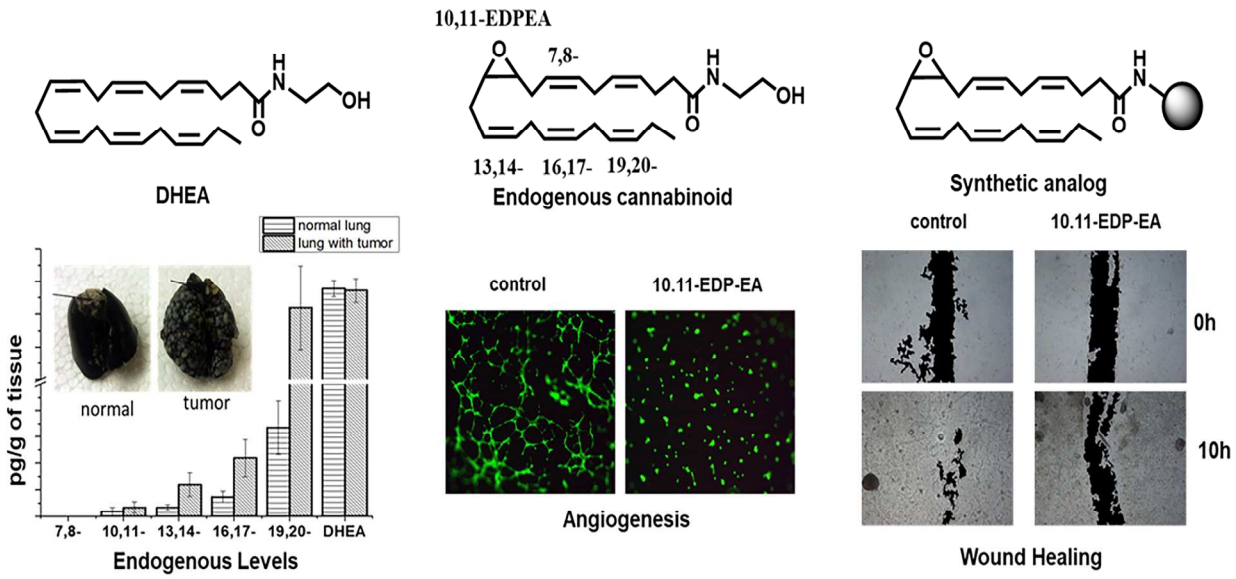

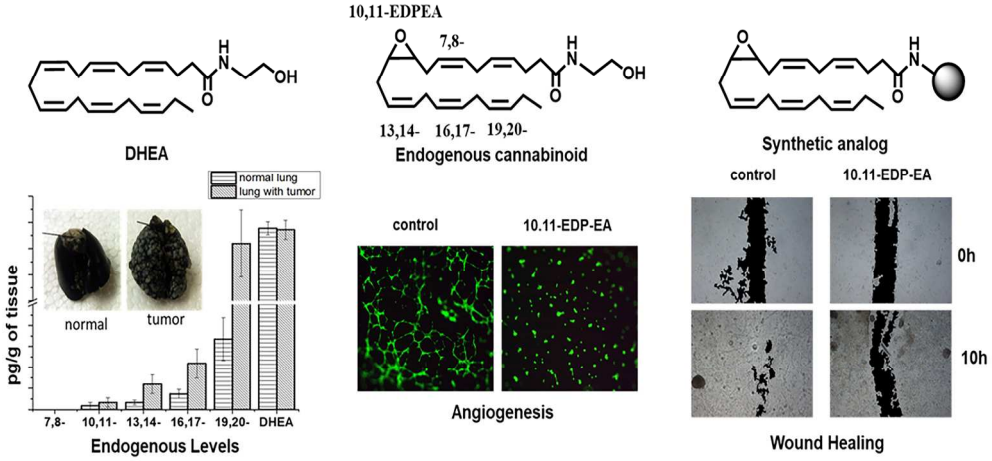

355x173mm (300 x 300 DPI)